LUND UNIVERSITY

Time-resolved x-ray spectroscopy of optical-field-ionized plasmas

Borgstrom, S; Fill, E; Starczewski, T; Steingruber, J; Svanberg, Sune; Wahlström, Claes-Göran

Link to publication

Total number of authors:
6

Time-resolved X-ray spectroscopy of optical-field ionized plasmas

S. Borgström[1], E. Fill[2], T. Starczewski[1], J. Steingruber[2], S. Svanberg[1], and C.-G. Wahlström[1]

[1]Department of Physics, Lund Institute of Technology, S-221 00 Lund, Sweden

[2]Max-Planck-Institut für Quantenoptik, D-85748 Garching, Germany

Abstract:

The time-dependent soft X-ray emission of helium and nitrogen plasmas generated by optical-field ionization is reported. The experiments were carried out by focusing pulses of the high-power Ti:sapphire laser of the Lund Institute of Technology ($\lambda = 796$ nm, pulse duration 150 fs, pulse energy 150 mJ) to a 50 μm diameter spot close to a nozzle, using He and N_2 as target gases. The emission on He^+, N^{4+} and N^{3+} resonance lines was recorded by means of a flat-field grating spectrometer coupled to an X-ray streak camera. A pronounced difference in the temporal shape of the emission of the Lyman-α line of hydrogen-like helium and of the 2p-3d resonance lines of lithium-like and beryllium-like nitrogen was observed. The helium line exhibited an initial spike followed by a slow revival of the emission, whereas the nitrogen lines showed a slow decay after a fast initial rise. These observations are explained with the help of simulations.

1. Introduction

The increasing availability of fs high-power laser systems has lead to a growing interest in the use of these lasers for the generation of plasmas. A convenient method to produce such plasmas takes advantage of the effect of optical-field ionization in which the high electric field of the laser pulse strips electrons from filled atomic shells (Perry et al. 1988; Augst et al. 1989). The interest in optical-field ionization derives from its relevance to atomic physics issues and from a possible application to X-ray lasers (Burnett and Corkum 1989, Amendt et al. 1991).

Under conditions in which the Keldysh parameter (Keldysh 1964)

$$\gamma = (U_q / 2U_p)^{1/2} \tag{1}$$

is < 1 the threshold intensity for producing an ion of charge q in the optical field of a laser pulse can be approximated by the classical expression (Augst et al. 1989, Penetrante and Bardsley 1991)

$$I_{th,q} = 4 \times 10^9 \frac{1}{q^2} U_q^4 \ . \tag{2}$$

The symbols in eqs (1) and (2) have the following meaning: U_q is the ionization potential of the ion with charge q-1 and $U_p = 9.33 \times 10^{-14} I \lambda^2$ is the ponderomotive potential (in eV) of an electron in a laser field with an intensity I (in W/cm^2) and wavelength λ (in μm).

Application of eq. (2) shows that an intensity around 10^{16} W/cm^2 is sufficient to generate ions of multiple charge. Helium, for example, is stripped to the bare nucleus and nitrogen from all of the electrons of its outermost shell, thus generating helium-like N^{5+}. The temperature of the generated electron gas depends on the polarization of the laser. For linearly polarized laser light low electron temperatures are predicted, as given by a combination of ATI heating and

inverse Bremsstrahlung (Penetrante and Bardsley 1991, Offenberger et al. 1993). The low electron temperature results in a high rate of recombination and, thus, optical field ionized plasmas emit radiation from ions of ionization stages lower than the initially generated one. The time-resolved emission in the direction of the laser beam consists of a short spike at the odd harmonics of the laser radiation, the duration of which is given by the laser pulse (Crane et al. 1992), whereas the emission of the ionic lines is determined by the recombination rate and lasts several ns.

In this work we present a study of the time resolved emission of helium and nitrogen ionic lines. Helium and nitrogen were chosen since they are relatively easily stripped to a parent ion, the lower ionization stage of which emits spectra which are simple and easy to analyze. Such investigations provide information about the plasma parameters after optical-field ionization and the subsequent evolution of the plasma.

2. Experimental setup

Linearly polarized laser pulses (λ = 796 nm, pulse duration 150 fs, pulse energy 150 mJ [Svanberg et al. 1993]) were focused into a pulsed gas jet emitted from a 800 μm diameter nozzle. With a lens of 50 cm focal length the beam was brought to a spot of approximately 50 μm diameter, yielding a peak intensity of about 5 x 10^{16} W/cm^2. With a backing pressure of 1 atmosphere the density in the gas jet 250 μm from the nozzle was about 10^{18} cm^{-3}, as measaured by an interferometric method (Faris and Hertz 1989, Altucci et al. 1995). The time-dependent emission of the lines in question was recorded in a longitudinal direction, by means of an X-ray streak camera coupled to a flat-field spectrometer. In order to obtain a high enough signal, up to 6000 shots were accumulated on the CCD readout. The time resolution of the system was essentially limited by the jitter of the streak camera, which was triggered from a fast photodiode exposed to part of the laser beam. By recording the emission on the 25th harmonic of the Ti:sapphire laser in argon (λ = 31.8 nm) the time resolution was determined to

3

be 100 ps (see fig. 1). A calibration of the time axis was obtained by delaying the streak camera trigger with cables of different length. The streak velocity was chosen to obtain a temporal window of about 3 ns duration.

3. Experimental results

A sufficient signal to noise ratio was obtained for the Lyman-α line of hydrogen-like helium (λ = 30.4 nm) and for the 2p-3d resonance line of lithium-like nitrogen (λ = 24.7 nm) as well as for several beryllium-like nitrogen 2p-3d lines. All of these lines had previously been observed with high intensity in time-integrated spectra under similar conditions (Borgström et al. 1994, Fill et al. 1995).

The time dependent intensity of He^+ Lyman-α is shown in fig. 2. It is striking that the emission consists of an initial peak with a duration of about 160 ps, followed by a minimum and a subsequent slow rise. To exclude the possibility of a spurious signal resulting from a harmonic, the experiment was repeated using transverse observation, which yielded the same result.

The emission of the He^+ Lyman-α line was recorded as a function of the backing pressure behind the the nozzle. Using the linear relationship between the reservoir pressure and the density in the gas jet (Perry et al. 1992) the applied pressures correspond to gas densities of 9.4×10^{17}, 7.2×10^{17}, 6.2×10^{17}, and 3.5×10^{17} cm^{-3} respectively. The absolute uncertainty is estimated to be about 30 %. The obtained emissions are displayed in figure 3. As the gas density is reduced, the general nature of the emission is unaltered, but the spike becomes less prominent and the rise of the emission gradually slows down.

For the nitrogen lines an initial spike as in helium was not observed. Instead, the emission started suddenly, with a rise time given by the time resolution of the system, and then gradually

decayed. Figures 4 and 5 display the time-dependent emission for the N^{4+} 2p-3d line at 24.7 nm and the N^{3+} 2s2p-2s3d transition at 28.4 nm. It is obvious that the beryllium-like line emission decays slower than the emission of the lithium-like line.

4. Comparison with simulations and discussion

The emission of the plasma on helium and nitrogen ionic lines was calculated with a computer code which takes into account ion kinetics and hydrodynamics after optical-field ionization. The code treats levels up to n = 6, simulating their evolution due to radiative and collisional transitions between each other and to the continuum. Hydrodynamic expansion is accounted for by means of a self-similar model (London & Rosen 1988, Dunne et al. 1994). The spatially integrated emission is calculated taking opacity effects into account. The limited time-resolution of the apparatus is included into the final result by convolving the original emission with a Gaussian function of 100 ps FWHM. "Standard" initial conditions are defined by an electron density $N_{e,0}$ as derived from the measured gas density and an electron temperature $T_{e,0}$ given by ATI heating, an assumption recently verified by Thomson scattering measurements (Offenberger et al. 1993, Glover et al. 1994). Note, however, that a higher electron temperature has been measured using time-of-flight spectroscopy (Mohideen et al. 1993). These "standard" initial conditions are $N_{e,0} = 2 \times 10^{18}$ cm^{-3} , $T_{e,0} = 40$ eV for helium and $N_{e,0} = 10^{19}$ cm^{-3}, $T_{e,0} = 20$ eV for nitrogen.

For helium it was found, that an initial spike as observed in the experiments, was not predicted by the simulations if the plasma was assumed to be initially fully ionized. Under this assumption only the slowly rising part of the emission was reproduced by the calculations, a feature resulting from the recombination of the plasma as it cools by hydrodynamic expansion.

However, if a small amount of the He^+ ions was assumed to be left in excited states after the laser pulse, a peaked emission quite similar to the experimental one was obtained. Figure 6

5

shows the result of a simulation of the helium Lyman-α emission if, as an initial condition, 1% of the total ion population was assumed in hydrogen-like helium states. The population was assumed to be distributed among the levels in a Boltzmann distribution with an excitation temperature of 40 eV. The figure shows, that this initial condition results in a predicted emission which resembles reasonably well the experimental one and also reproduces its density dependence. A number of runs with different parameters were carried out to determine the sensitivity of the calculated emission to variations in the initial conditions. It was found that the assumption of a small amount of He^+ ions in the ground state (and no population in excited levels) did not result in an emission similar to the experimental one. It was further verified, that the temporal shape of the calculated emission was quite sensitive to the amount of ions assumed to be in hydrogenic levels: The spike was too small if only 0.5 % of the ions were in hydrogenic levels and it was considerably more dominant than in the experiment if that fraction was > 1.5 %.

These calculations suggest that in helium a small fraction of the population is left in excited states of the hydrogen-like He^+ ion after optical-field ionization. This result may be due to the spatially integrated nature of the observed emission, indicating that in the outer region of the focused laser beam, where the field strength is sufficiently low, excited He^+ ions exist. Another explanation invokes the effect of "stabilization" in an intense laser field: It is well-known that several mechanisms can impede ionization in high electric fields. The corresponding effect has been predicted on quantum-mechanical grounds (Pont and Gavrilla 1990, Bucksbaum and Jones 1992) and experimentally observed in Ba^+ ions (Jones and Bucksbaum 1991).

For the N^{4+} 2p-3d line the temporal shape of the emission predicted by the simulations agreed quite well with the experimental one if "standard" initial conditions (and no population in Li-like excited states) were assumed (see fig. 7). Surprisingly, however, a short spike appears in the calculated emission, which is caused by the fact that the 2p-3d line is optically thin in the initial phase of the recombination, but gradually becomes strongly absorbing as more and more ions accumulate in the lithium-like ground state. The reason, why such a spike is not

observed in the experiment is not clear, but may be due to population left in the lithium-like ground state after the laser pulse, which prevents the line from being optically thin. It should be mentioned that the helium spike cannot be explained by an opacity effect, due to the lower ion density (by a factor of two) and the larger line width of the He^+ Lyman-α line.

The emission on the beryllium-like 2p-3d nitrogen line was not simulated, because of the difficulty in modelling the multitude of levels of beryllium-like ions. Qualitatively, however, the following conclusions can be reached about the beryllium-like emission: If the radiating ions were generated by sequential recombination from the helium-like through the lithium-like stage, the emission would exhibit a slow rise, caused by the gradual accumulation of ions in the lithium-like ground state. The fact that we see a fast rise with a subsequent slow decay indicates, that the observed beryllium-like emission originates from a region of lower intensity, in which low ionization stages are present immediately after the laser pulse.

5. Conclusion

The time-resolved emission of He^+, N^{3+} and N^{4+} resonance lines after optical-field ionization with a fs laser pulse was recorded. The time history of the emission in helium and nitrogen was found to be quite different. In helium an initial peak followed by a slow rise was observed, whereas in nitrogen no such peak but a slow decay after an initial fast rise was seen. Simulations using appropriate initial conditions of the electron density and temperature of the plasma after optical field ionization result in a satisfactory agreement with the observations. For helium, modifications to the "standard" initial conditions must be made which involve the assumption of an excited state population in He^+ levels. For N^{4+} "standard" initial conditions reproduce the observed emission except for a short initial spike not seen in the experiments.

7

supported by the Swedish National Science Research Council and was performed within the framework of the European X-ray Laser Network.

REFERENCES

Altucci, C. et al. 1995, to be published.

Amendt, P., Eder,D.C. & Wilks, S.C. 1991 *Phys. Rev. Lett.* **66**, 2589.

Augst, S. et al. 1989 *Phys Rev. Lett.* **63**, 2212.

Borgström, S. et al 1994 *Proc. 4th International Coll. X-ray Lasers,* Williamsburg, Virginia, May 1994

Bucksbaum, P.H. & Jones, R.R. "Stability of atoms in intense laser fields" 1992 *AIP Conf. Proc.* **275**, Atomic Physics 13, edited by H. Walther, T.W. Hänsch and B. Neizert, Munich 1992.

Burnett, N.H. & Corkum, P.B. 1989 *J. Opt. Soc. Am.* **B 6**, 1195.

Crane, J.K. et al. 1992 *Opt. Lett.* **17**,1256.

Dunne, M. et al. 1994 *Phys. Rev. Lett.* **72**, 1024.

Faris, G.W. & Hertz, H.M. 1989 *Appl. Opt.* **28**, 4662.

Fill, E. et al. 1995, to be published.

Glover, T.E. et al. 1994 *Phys. Rev. Lett.* **73**, 78.

Jones R.R. & Bucksbaum, P.H. 1991 *Phys. Rev. Lett* **67**, 3215.

Keldysh, L.V 1964 *Zh. Exp. Teor. Fiz.* **47**, 1945.

London, R.A. & Rosen, M.D. 1986 *Phys. Fluids* **29**, 3813.

Mohideen U. et al. 1993 *Phys. Rev. Lett.* **71**, 509.

Offenberger, A.A. et al. 1993 *Phys. Rev. Lett.* **71**, 3983.

Penetrante, B.M. & Bardsley J.N. 1991 *Phys. Rev.* **A 43**, 3100.

Perry, M.D. et al. 1988 *Phys. Rev. Lett.* **60**, 1270.

Perry, M.D. et al. 1992 *Opt. Lett.* **17**, 523.

Pont, M. & Gavrilla, M. 1990 *Phys. Rev. Lett.* **65**, 2362.

Svanberg, S. et al. 1994 *Phys. Scripta* **49**, 187.

FIGURE CAPTIONS

Fig. 1: Recording of 25th harmonic of Ti:sapphire laser ($\lambda = 31.8$ nm) generated in argon. The diagram demonstrates the time-resolution of the detection system.

Fig. 2: Temporal shape of the He^+ Lyman-α emission ($\lambda = 30.4$ nm) showing initial spike and subsequent revival. The nominal gas density for this recording was 7.2×10^{17} cm^{-3}.

Fig. 3: Temporal shape of He^+ Lyman-α emission for different gas densities.

Fig. 4: Time-dependent emission of N^{4+} 2p-3d line ($\lambda = 24.7$ nm). Gas density 10^{18} cm^{-3}.

Fig. 5: Time dependent emission of N^{3+} 2s2p-2s3d transition ($\lambda = 28.4$ nm). Gas density 10^{18} cm^{-3}.

Fig. 6: Simulation of He^+ Lyman-α emission at different gas densities. $T_e = 40$ eV; 1 % of the initial ion population in He^+ ionic levels.

Fig. 7: Simulation of N^{4+} 2p-3d emission. "Standard" initial conditions ($N_e = 10^{19}$ cm^{-3}, $T_e = 20$ eV).

intensity (arb. u.)
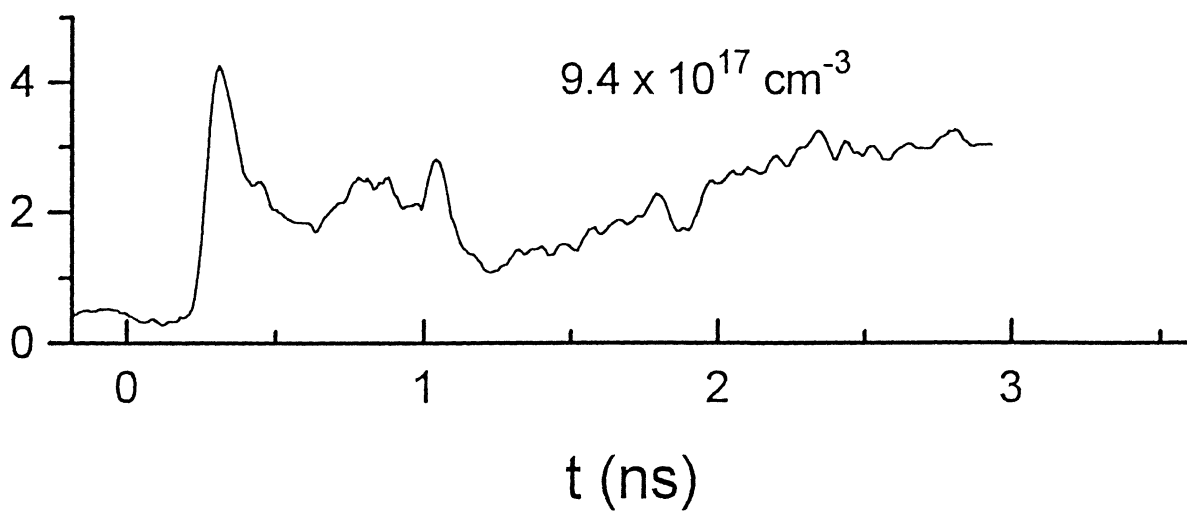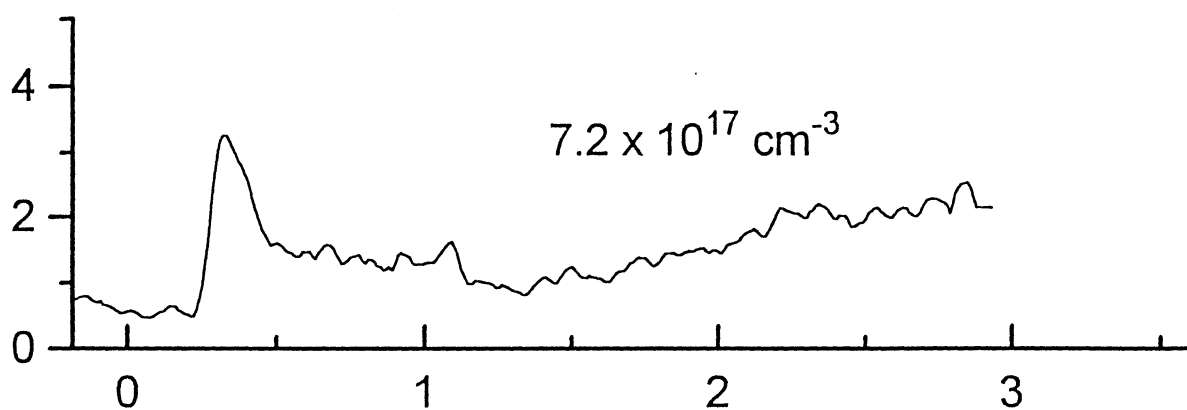
t (ns)

Fig. 1

Fig. 2

$N_{gas} = 3.5 \times 10^{17}\ cm^{-3}$

$6.2 \times 10^{17}\ cm^{-3}$

$7.2 \times 10^{17}\ cm^{-3}$

$9.4 \times 10^{17}\ cm^{-3}$

t (ns)

intensity (arb. u.)

N⁴⁺ 2p-3d

t (ns)

fig. 4

intensity (arb. u.)

t (ns)

N³⁺ 2s2p-2s2p

fig. 5

Fig.6

intensity (arb. u.)

t (ns)

N^{4+} 2p-3d emission
$N_e = 10^{19}$ cm^{-3}
$T_e = 20$ eV
100 ps time resolution

fig. 7